Environ Sci Pollut Res (2016) 23:12739–12754
DOI 10.1007/s11356-015-4997-2

Ecosystem functioning approach applied to a large contaminated coastal site: the study case of the Mar Piccolo of Taranto (Ionian Sea)

Tamara Cibic[1] · Lucia Bongiorni[2] · Flavio Borfecchia[3] · Antonella Di Leo[4] · Annalisa Franzo[1] · Santina Giandomenico[4] · Ana Karuza[1] · Carla Micheli[3] · Manja Rogelja[1,5] · Lucia Spada[4] · Paola Del Negro[1]

Received: 31 March 2015 / Accepted: 30 June 2015 / Published online: 11 July 2015

Abstract Knowledge on ecosystem functioning can largely contribute to promote ecosystem-based management and its application. The Mar Piccolo of Taranto is a densely populated area at a high risk of environmental crisis. Here, planktonic primary production (PP) and heterotrophic prokaryotic production (HPP) were measured as proxies of functioning in three sampling sites located in two inlets at different levels of industrial contamination, during three sampling surveys (June 2013, February and April 2014). To have a better overall view and provide some insights into the benthic-pelagic coupling, we integrated PP and HPP in the water column with those in the sediments and then discussed this with the origin of the organic matter pools based on analysis of stable isotopes. Heavy metals and polychlorobiphenyls (PCBs) were also analysed in the surface (1 cm) sediment layer and related to the overall ecosystem functioning. Multidimensional scaling (MDS) analysis, based on the main data, clearly separated the second inlet from the first one, more severely impacted by anthropogenic activities. The stable isotope mixing model suggested the prevalent terrestrial/riverine origin of the particulate organic matter pools (mean 45.5 %) in all sampling periods, whereas phytoplankton contributed up to 29 % in February. Planktonic PP and HPP rates followed the same pattern over the entire study period and seemed to respond to phytoplankton dynamics confirming this community as the main driver for the C cycling in the water column. On the contrary, benthic PP rates were almost negligible while HPP rates were lower or comparable to those in the water column indicating that although the Mar Piccolo is very shallow, the water column is much more productive than the surface sediments. The sediment resuspension is likely responsible for a pulsed input of contaminants into the water column. However, their interference with the proper functioning of the pelagic ecosystem seems to be limited to the bottom layers.

Responsible editor: Philippe Garrigues

Electronic supplementary material The online version of this article (doi:10.1007/s11356-015-4997-2) contains supplementary material, which is available to authorized users.

✉ Tamara Cibic
tcibic@ogs.trieste.it

[1] OGS (Istituto Nazionale di Oceanografia e di Geofisica Sperimentale), Sezione Oceanografia, Via A. Piccard 54, 34151 Trieste, Italy

[2] CNR—Istituto di Scienze Marine (ISMAR), Arsenale—Tesa 104, Castello 2737/F, 30122 Venezia, Italy

[3] ENEA Research Center Casaccia Roma, C.P. 2400/00123S. Maria di Galeria, Roma, Italy

[4] Consiglio Nazionale delle Ricerche (CNR), Istituto per l'Ambiente Marino Costiero—IAMC, 74123 Taranto, Italy

[5] Università di Trieste, Department of Life Sciences, 34127 Trieste, Italy

Keywords Ecosystem functioning · Primary production · Heterotrophic prokaryotic production · C and N stable isotopes · Benthic-pelagic coupling · Contamination · Satellite imagery mapping

Introduction

Shallow coastal photic systems are among the most productive on the planet (Odum 1983). In these environments, light penetration to the bottom fuels multiple primary producers, including phytoplankton, benthic microalgae, macroalgae and seagrasses.

The coupling between planktonic primary production (PP) and prokaryotic utilization of the labile, i.e. rapidly decomposable, phytoplankton extracellular release has been demonstrated to be a key process in organic carbon cycling influencing the ecosystem functioning in aquatic ecosystems (Cole et al. 1988). Heterotrophic prokaryotes mainly consume and respire organic matter produced by photosynthesis; therefore, heterotrophic prokaryotic production (HPP) is typically dependent on this organic matter supply. However, the coupling between PP and HPP may vary according to the ecosystem characteristics. For example, in estuarine and coastal systems, the prokaryotic C demand could be supported not only by the degradation of phytoplankton exudates but also by local non-phytoplanktonic material and allochthonous organic matter supplies (Lee et al. 2001). This can be reflected in a loose coupling between PP and HPP and a shift to net heterotrophy of the planktonic system (Pugnetti et al. 2005, 2010).

Aside from light, temperature and nutrients, that are key parameters regulating system production, coastal processes are largely influenced by physical factors such as horizontal transport, sediment composition and resuspension. Rapid sinking of phytoplankton blooms, efficient filtration of the water column by benthic fauna and a tidal energy subsidy can determine a tight benthic-pelagic coupling that leads to a high local benthic production (Kennish et al. 2014). Moreover, microbial-mediated processes in sediments can enhance nutrient availability for primary production in benthic and pelagic habitats and become important in regulating the relative magnitude of benthic versus pelagic primary production (Kennish et al. 2014). Apart from phytoplankton and local benthic production, terrestrial matter carried by coastal rivers represents a non-negligible contributor to coastal organic matter pools.

The understanding of the nature and origin of the organic matter pools may provide interesting insights about the occurrence of natural processes and anthropogenic pressures in coastal environments (Hedges and Stern 1984). At this regard, analyses of stable isotopes of organic matter are useful tools to characterize nitrogen and carbon transport and transformation processes in continental margins (Sanchez-Vidal et al. 2009).

Shallow coastal photic systems rank among the most heavily impacted aquatic ecosystems, being affected by a wide range of anthropogenic activities. Multiple anthropogenic disturbances create both acute and insidious problems for many estuarine biotic communities and habitats that can compromise the stability and resiliency of these systems and their long-term integrity. Among other stressors, chemical contaminants can cause severe changes in ecosystem structure and function (Kennish et al. 2014).

Regarding organic pollutants and particularly polychlorinated biphenyls (PCBs), current sources of these compounds are landfills, open burning of products containing PCBs, waste incineration, accidental fires and revolatilization from formerly exposed soils. Organic pollutants enter the sea and estuary via atmospheric deposition, river input and point source along the coast. Once delivered to the water column, the primary removal processes are sedimentation of atmospheric particles and partitioning of the gaseous/dissolved phase contaminants into organic carbon-rich particles with subsequent settling and accumulation in surface sediments (Di Leo et al. 2014).

The main process determining the distribution and concentration of contaminants in shallow systems is the exchange between the water column and the uppermost sediment layer that is repeatedly resuspended and settled again. In this way, contaminants are transferred to the water column, diluted and redistributed over the entire basin through water circulation. Usually, for monitoring purposes, analysis of contaminants is performed on a sediment layer up to 5 cm (Cardellicchio et al. 2007). However, focusing on the benthic-pelagic coupling, it is important to estimate the contaminant concentrations in the uppermost few millimetres of sediments that are often resuspended.

The Mar Piccolo is a shallow coastal basin located near the city of Taranto (Southern Italy). Since 1960s, Taranto and its coastline have been subjected to the industrialization process that has caused profound environmental changes. This industrial zone is characterized mainly by the presence of the largest steelworks in Europe and navy arsenal in Italy (military area in Fig. 1), a major oil refinery, shipbuilding and other industrial activities that are responsible for severe environmental contamination, mainly due to heavy metals, asbestos, polycyclic aromatic hydrocarbons (PAHs), organic solvents, PCBs and dioxin. Previously collected data on organic and inorganic pollutants in the Mar Piccolo have shown high levels of contamination and stress conditions on different communities (Cardellicchio et al. 2007; Spada et al. 2012). In 1998, this area has been declared Site of National Interest (SIN), i.e. a very large contaminated area, classified as the most dangerous by the Italian State and in need of remediation. According to the current legislation, the characterization plan of such polluted areas is based solely on the quantification of contaminants. In contrast, other pivotal ecological aspects, such as those focused on the C cycling through the production processes, have been completely neglected.

The principle behind "the ecosystem approach to management" is that the management of human activities is based on the limits within which ecosystem structure, functioning, productivity and biological diversity can be maintained (Ottersen et al. 2011). There are still major science and knowledge gaps in applying the ecosystem approach to management, related to our limited understanding of the dynamics and resilience of ecosystems, the cumulative impacts of human uses on the marine environment and the effectiveness of management and governance systems (Katsanevakis et al. 2011). To study the ecosystem functioning of a particular environment, as much information as possible have to be gathered on that area. The simultaneous investigation of structural

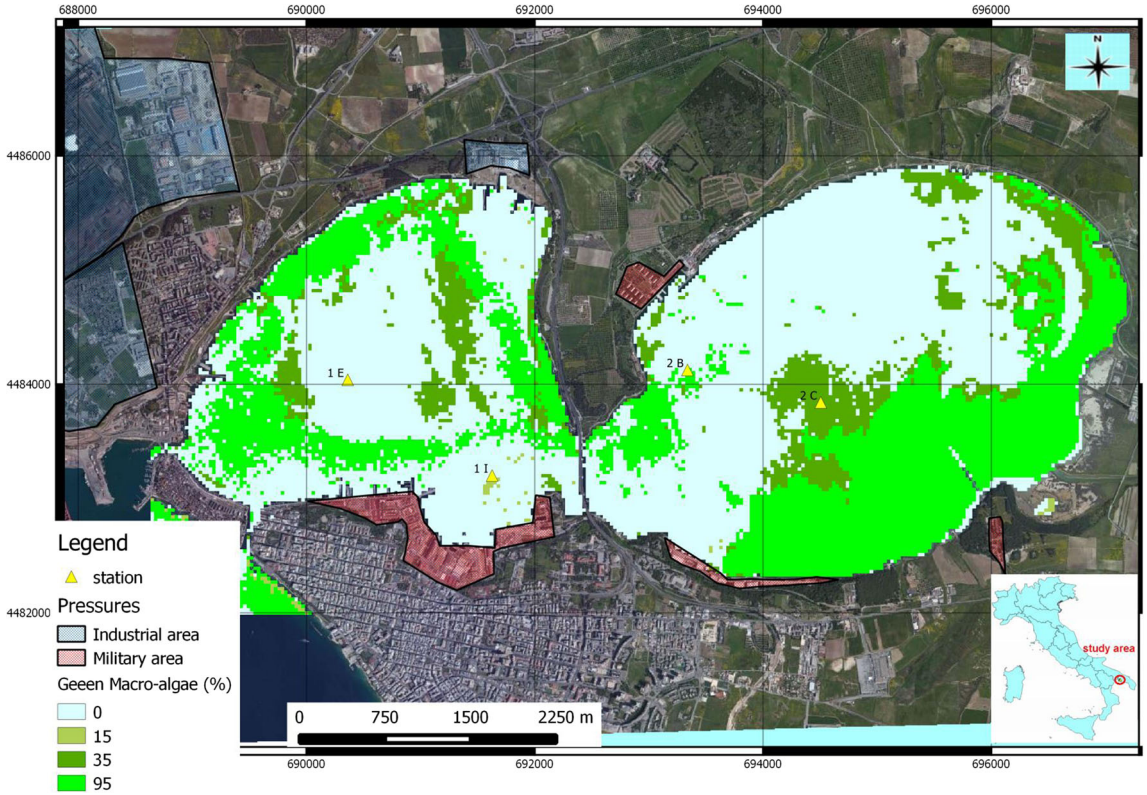

Fig. 1 Location of the four sampling stations in the Mar Piccolo of Taranto (*yellow triangles*): 1I and 1E in the first inlet and 2B and 2C in the second inlet. Superimposed are the industrial area and the military area (i.e. the navy arsenal in the first inlet) and the green macroalgal coverage (%). Its distribution was assessed by means of atmospherically corrected Landsat 8 OLI multispectral data acquired on 13 June 2013 and suitably calibrated using in situ point measurements at the sampling stations

and functional parameters and their subsequent integration is needed in order to represent an overview of the C flow through the system. In the Mar Piccolo of Taranto, there are no data available on either PP or HPP that are considered important proxies of ecosystem functioning. In this study, we have focused on the pelagic processes of carbon production. To gain more insights into the ecosystem functioning and the influence of pelagic-benthic and import/export processes, we have (i) integrated the PP and HPP in the water column with those in the benthic domain and (ii) linked such information with the nature and origin of suspended and sedimentary organic matter (OM) pools based on analyses of stable isotopes ($\delta^{13}C$ and $\delta^{15}N$). Moreover, we discussed the high contamination levels in the very uppermost sediment layer, their transfer to the water column through bottom resuspension and the consequent potential effects on the overall ecosystem functioning of this basin.

Materials and methods

Study area

The Mar Piccolo is a shallow, nearly enclosed basin connected through two narrow canals with the Mar Grande and widely with the Gulf of Taranto. It consists of two naturally divided basins, the first and second inlet, with maximum depths of 13 and 10 m and a surface area of 8.28 and 12.43 km^2, respectively. The sedimentation in this area is mainly influenced by land run-off, numerous submarine springs, small streams, sewage outfalls and industrial discharges rather than by marine currents. The sediment composition in both inlets is clayey silt. The features of the Mar Piccolo in the Gulf of Taranto have been exhaustively described by Cardellicchio et al. (2015 this issue).

Sampling

Sampling in the water column was carried out during 11–17 June 2013, 3–5 February and 1–8 April 2014 at three stations: St. 1E (depth=11.2 m) was located in the middle of the first inlet (40° 29′ 01″ N, 17° 14′ 46″ E), St. 1I (depth=11.0 m) was located nearby the military arsenal (40° 28′ 46″ N, 17° 15′ 38″ E), and St. 2C (depth=8.0 m) was positioned in the innermost part of the second inlet (40° 28′ 57″ N, 17° 17′ 41″ E) (Fig. 1).

Seawater temperature, dissolved oxygen and salinity were measured along the water column using a Seabird 19 Plus Seacat probe (June 2013 and April 2014) whereas in February 2014, seawater temperature was measured by a

PNF-300 Profiling Natural Fluorometer and salinity by a CDM83 conductivity meter (Radiometer Copenhagen).

During each sampling, the photosynthetic available radiation (PAR) was registered by a PNF-300 Profiling Natural Fluorometer (Biospherical Instruments Inc.). The PAR value at the sampling depth was expressed as the percentage of measured irradiance with respect to the surface irradiance (%PAR).

Water samples were collected at the surface layer (1 m below water surface) and bottom layer (1 m above bottom) by Niskin bottles. For isotopic analyses of suspended particulate organic matter (POM), water samples were collected from the bottom layer of the three stations listed above and at the additional St. 2B (depth=7.0 m; 40° 28′ 57″ N, 17° 16′ 42″ E) located nearby the strait between the two inlets. Replicated water samples (1–1.2 L) were filtered through precombusted (450 °C for 4 h) Whatman GF/F filters and stored at −20 °C until analyses.

Sediment sampling was carried out in June 2013 and April 2014 at the four stations sampled for water analyses. At each station, at least three virtually undisturbed sediment cores were collected by scuba divers using polycarbonate sample tubes (12.7 cm ID with a sample area of 127 cm^2). The oxic sediment layer (0–1 cm ca.) of each core was collected, homogenized and used for the analysis of heavy metals and PCBs (see below) as well as primary and heterotrophic productions (as reported in Rubino et al. (2015 this issue) and Franzo et al. (2015 this issue), respectively).

Additional sediment samples (0–3 cm layer) were used to analyse the stable isotopic signatures of sedimentary organic matter (SOM) as described in Bongiorni et al. (2015 this issue). For this analysis, an additional sampling was carried out in February 2015. In order to characterize the contribution of different primary sources to POM and SOM pools, most common macroalgal species were also collected during June 2013 and April 2014 by hand or a van Veen grab (as reported in Bongiorni et al. (2015 this issue)).

Chlorophyll a

Water subsamples for chlorophyll *a* (chl *a*) analysis were collected on-board, stored in the dark and kept at 4 °C until the filtration. In the laboratory, the water was filtered immediately on 47 Ø mm Whatman GF/F filters and the filters were stored at −20 °C. Chl *a*, corrected for phaeopigments, was measured fluorometrically after extraction (90 % acetone) and centrifugation of samples kept in the dark, according to Lorenzen and Jeffrey (1980), on a Perkin Elmer LS50B fluorometer.

Primary production

PP was estimated in situ by the ^{14}C technique (Steemann-Nielsen 1952). Water samples were poured into 75-mL translucent and dark polycarbonate carboys (Nalgene) and kept in the darkness for 30 min to stop the residual photosynthetic activity. Subsequently, 6 μCi (0.22 MBq) of $NaH^{14}CO_3$ (DHI, Denmark) was added per bottle. Three light and one dark samples per depth were fixed on a rosette, lowered at the corresponding depth and incubated for 2 h around noon. At the end of the incubation, samples were transferred to 100-mL bottles and supplemented with 320 μL of 5 N HCl (Cibic and Virgilio 2011) to stop the photosynthetic activity and remove the residual labelled bicarbonate, not assimilated by the phototrophic plankton. From each sample, 25 mL were filtered through polycarbonate 0.2 μm filters (Nuclepore) applying a low vacuum pressure (5 mmHg) in order to avoid cell damage. Filters were placed into 6-mL plastic scintillation vials (Perkin Elmer), and 5 mL of Filter Count scintillation cocktail (Perkin Elmer) was added. Disintegrations per minute (DPM) were measured by a QuantaSmart TRI-CARB 2900 TR Liquid Scintillation Analyzer (Packard BioScience, USA) including quenching correction, obtained using internal standards. Assimilation of carbon was calculated as described by Gargas (1975), assuming 5 % isotope discrimination. Activity of the added $NaH^{14}CO_3$ and inorganic carbon concentration (tCO_2) were calculated on the basis of total alkalinity measured in the same samples.

Similarly to the water column, benthic PP was estimated using ^{14}C as radiotracer. ^{14}C incubation of sediment slurries was performed in situ; then, samples were treated and analysed as described in detail by Cibic et al. (2008).

Heterotrophic prokaryotic production

HPP was measured by the incorporation of ^{3}H-leucine (Leu) (Kirchman et al. 1985). Triplicate seawater aliquots (1.7 mL) and two controls killed by the addition of 90 μL 100 % trichloracetic acid (TCA) were amended with a 20-nM radiotracer and incubated in situ in the dark. Incubations were stopped with TCA (5 % final concentration) after 2 h. The extraction with 5 % TCA and 80 % ethanol was carried out using the microcentrifugation method (Smith and Azam 1992). Activity in the samples was determined by a QuantaSmart TRI-CARB 2900 TR Liquid Scintillation Analyzer (Packard BioScience, USA) after the addition of 1 mL scintillation cocktail (Ultima Gold MV; Perkin Elmer).

Benthic heterotrophic production was measured by the incorporation of ^{3}H-leucine following the method by Manini et al. (2004). ^{3}H incubation of sediment slurries was performed in situ, and then, samples were treated and analysed as exhaustively described by Cibic et al. (2012).

Stable isotope analysis

Analyses of C and N stable isotopes ($\delta^{13}C$ and $\delta^{15}N$) of POM and SOM and primary producers were conducted as detailed

in Bongiorni et al. (2015 this issue). Briefly, $\delta^{13}C$ was analysed after acidification with HCl (1 N) to remove carbonates which present a higher $\delta^{13}C$ than organic carbon (Hedges and Stern 1984) while $\delta^{15}N$ was analysed without any prior treatment. The $\delta^{13}C$ and $\delta^{15}N$ ratios in the samples were determined using a Delta Plus XP isotope ratio mass spectrometer (ThermoFinnigan) equipped with a Flash EA 1112 elemental analyser (ThermoFinnigan). Ratios were expressed as parts per thousands (‰) differences from a standard reference material VPDB (Vienna Pee Dee Belemnite) for $\delta^{13}C$ and AIR for $\delta^{15}N$. The uncertainty of methods was 0.3‰ for $\delta^{13}C$ and δ^{15} N.

In order to evaluate the contribution of different primary sources to the POM and SOM mix pools, we applied a Bayeasian mixing model by using the package SIAR V4 (Stable Isotope Analysis in R, (Parnell et al. 2010)). The greatest advantage of this procedure is the incorporation of uncertainty linked to sources, consumers and trophic enrichment factors within the model (Dubois et al. 2012; Parnell et al. 2010; Phillips et al. 2014). The model was run for POM and SOM separately and for each of the four sampling stations/seasons assuming a zero fractionation factor for each isotopes. Both models included two variables ($\delta^{15}N$ and $\delta^{13}C$) and up to five end-members (macroalgae, terrestrial/riverine POM, phytoplankton, treated sewage for POM and SOM models and autochthonous POM for SOM model). Due to similar signature of different macroalgal species, only the average isotopic value was used in the model (−16.83±2.49 and 10.45±1.27 for $\delta^{13}C$ and $\delta^{15}N$, respectively). The isotopic values of the end-members that were not directly measured during our surveys were extracted from the literature: phytoplankton (Harmelin-Vivien et al. 2008, −19.95±0.93 and 4.50±0.80 for $\delta^{13}C$ and $\delta^{15}N$, respectively), riverine/terrestrial POM (Berto et al. 2013 and Carlier et al. 2007, −25.58±0.67 and 2.92±0.45 for $\delta^{13}C$ and $\delta^{15}N$, respectively) and treated sewage (Berto et al. 2013 and Berto unpubl. data, −24.76±0.88 and 19.11±3.92 for $\delta^{13}C$ and $\delta^{15}N$, respectively).

Satellite imagery mapping of the seabottom and primary productivity of green algae

The green macroalgal distribution in the Mar Piccolo of Taranto was assessed by means of the high-resolution multispectral satellite remote sensing technique based on the data acquired on 13 June 2013 by the new NASA polar Landsat 8 Operational Land Imager (OLI) sensor. The OLI multispectral data were previously corrected for atmospheric noise (Borfecchia et al. 2013a) (scattering/attenuation from image derived AOD and adjacency effects), and then, they were classified into three classes using a supervised maximum likelihood (ML) parametric algorithm. Different in situ cover values (%) of the dominant green algae *Caulerpa* sp., recorded at the four stations in the same period, allowed us to properly calibrate the remotely sensed data. The improved spectral and radiometric features of the OLI multispectral sensor (five acquisition bands in the VIS and NIR ranges including the new deep blue coastal one, at 30 m resolution with increased SNR) allowed us to obtain these preliminary results in terms of green algae effective mapping (Borfecchia et al. 2013b) in the optically complex shallow waters of the Mar Piccolo. The primary productivity of green macroalgae (such as *Caulerpa prolifera*, *Caulerpa* sp.) in the Mar Piccolo was evaluated through an integrated method including satellite remote sensing technique and in situ observations. In order to obtain an estimate of the overall primary productivity of the Mar Piccolo, a maximum hourly rate of productivity (P_{max}) of *Caulerpa* sp., in relation to depth and seasonal variation, was used according to Terrados and Ros (1992) and Bernardeau-Esteller et al. (2011) and converted from oxygen to carbon to allow an integration with primary production data in the water column.

Analysis of polychlorobiphenyls and heavy metals

PCBs congener IUPAC No PCB 18, 31, 28 (tri-CBs), 44, 52 (tetra-CBs), 95, 101, 99, 110, 123, 118, 114, 105 (penta-CBs) 151, 149, 146, 153, 138, 128, 167, 156, 157 (hexa-CBs) and 187, 183, 177, 180, 170, 189 (hepta-CBs) (Ultra Scientific, Co.) in lyophilized sediments were extracted with *n*-exane/acetone (1:1 *v*/*v*) by microwave extraction (EPA Method 3546), purified with Florisil (EPA Method 3620C) and analysed by GC-MS (EPA method 8082A).

Metals (As, Cd, Cr, Cu, Fe, Ni, Zn, Pb, Al, V, Mn, Sn, Hg) in lyophilized sediments were digested with 9 mL of nitric acid, 2 mL of hydrochloric acid and 3 mL of hydrofluoric acid (SW-846 EPA Method 3052, 1995) using a MARSX microwave oven and analysed by ICP-MS. For a more detailed explanation of the protocols for PCBs and metal analyses, see Di Leo et al. (2015 this issue).

Statistical analysis

Data normality was checked by Shapiro-Wilk's test. Mean HPP and PP data and values of surface and bottom layers were compared by Mann-Whitney *U* test. In order to highlight differences in PP, HPP and stable isotopes among sampling months and stations, one-way and two-way ANOVA were applied. Prior to analyses, the heterogeneity of variance was tested using Cochran's C test, and when the assumption was not reached, data were appropriately transformed. When significant differences were observed, means were compared using a Tukey's HSD test. To highlight interactions between structural and functional variables, the non-parametric Spearman's rank correlation analysis (R) was applied. All analyses including the Bayesian stable isotope mixing model (SIAR V 4 package) were performed using the R software.

Multidimensional scaling (MDS) analysis was performed using PRIMER software v.5 on bottom and surface data separately. The two data matrices were constructed with three replicate samples of PP and HPP rates and were implemented with structural biological parameters such as the abundances of picoplankton (both heterotrophic and autotrophic fractions) and nanophytoplankton (data from Karuza et al. 2015 this issue). Stable isotope data ($\delta^{15}N$ and $\delta^{13}C$ signature of POM) were included only in the bottom layer dataset. Normalized Euclidean distance was applied. Variation in trends among sampling periods, inlets and stations was subsequently tested for significance with an analysis of similarity (ANOSIM) using the same software. ANOSIM tests a priori-defined groups (subgroupings based on the abovementioned factors) against random groups in ordinate space. A 0 indicates that there is no difference among groups, while 1 indicates that all samples within groups are more similar to one another than any samples from different groups. Only statistically significant data are presented.

Results

Physical-chemical parameters in the water column

At the three sampling stations, temperature varied between 20.9 and 23.5 °C in June and between 15.5 and 17.0 °C in April, whereas no thermocline was registered in February (Table 1). The water column displayed oxygen saturation conditions both in June and April, reaching 124.6 % at the bottom layer of the second inlet in April. A strong halocline was observed in all sampling periods, with differences of up to 3.7 between the surface and the bottom layers (measured in the center of the first inlet during February), probably due to surface freshwater inputs. During all sampling periods, PAR irradiance was never a limiting factor for the phototrophic organisms; the lowest values did not drop below 22.6 $\mu Em^{-2}\ s^{-1}$ at the bottom layer in February, representing 4.9 % of the surface PAR. Phaeo/chl *a* ratio showed low values in June (with the exception of the surface layer at St. 2C) and in April indicating the presence of fresh produced organic matter of phytoplankton origin.

Primary and heterotrophic prokaryotic production

Planktonic PP was always significantly higher at the surface than at the bottom water layer (Mann-Whitney *U* test, $U=587$, $p<0.001$). The only exception occurred in April in the second inlet, where not significant differences between the two layers were found. The two-way ANOVA highlighted differences in PP of the surface layer between seasons and sampling stations ($F_{2,18}=200.70$ and $F_{2,18}=20.3$, $p<0.001$, respectively). Similar results were obtained for PP at the bottom layer ($F_{2,18}=841.83$ and $F_{2,18}=141.47$, $p<0.001$). At both surface and bottom layers, with the only exception of February, higher values were consistently recorded at St. 2C (Tukey's HSD, $p<0.01$). The highest PP values were obtained in June, when hourly rates varied between 2.82±0.10 μg C L^{-1} h^{-1} at the bottom of St. 1I and 20.07±3.12 μgC L^{-1} h^{-1} at the surface of St. 2C (Fig. 2).

The Mar Piccolo was productive also in February, i.e. in lower light conditions, with values up to 3.22±0.14 μg C L^{-1} h^{-1} at the surface layer of the first inlet. Intermediate rates were estimated in April, varying between 1.20±0.14 μg C L^{-1} h^{-1} at the surface of St. 1I and 6.71±0.91 μg C L^{-1} h^{-1} at the bottom of the second inlet. In June and April, chl *a*-normalized photosynthetic rates displayed quite a different pattern compared to the not normalized rates. At the bottom layers of the three stations, the two rates were rather comparable, whereas at the surface layers PP chl^{-1} values were about half of the not normalized rates (Table 2).

In February, except for the surface layer of St. 1I, where a higher PP chl^{-1} rate was calculated, comparable PP normalized and not normalized rates were obtained. Mean PP values were calculated from data collected at the two depths along the water column to obtain the areal phytoplankton production (PPa). At the shallowest St. 2C, PPa rates displayed the highest variability, ranging from 1.20 mg C m^{-2} h^{-1} in February to 12.62 mg C m^{-2} h^{-1} in June and representing the absolute minimum and maximum of the study period. With the exception of February, higher PP areal rates were obtained in the second inlet.

PP was always higher than HPP ($U=324$, $p<0.001$). The HPP rates in the water column displayed quite similar patterns to those observed for the PP (Fig. 2). HPP rates resulted regularly higher at the surface than at the bottom depth ($U=554$, $p<0.01$); only at St. 2C in April, no difference was observed between the sampling depths.

The two-way ANOVA highlighted differences in the HPP rates of the surface and bottom layers between seasons and sampling stations ($F_{2,18}=491.46$ and $F_{2,18}=252.91$, $p<0.001$ for surface layers and $F_{2,18}=695.02$ and $F_{2,18}=131.14$, $p<0.001$ for bottom layers, respectively). The highest HPP rates were detected in June (Tukey's HSD, $p<0.01$), always exceeding 0.72±0.01 μg C L^{-1} h^{-1} at the surface and 0.32±0.01 μg C L^{-1} h^{-1} at the bottom. At St. 2C, the HPP rates were always higher than at the other sampling stations (Tukey's HSD, $p<0.01$) and reached the maximum value (2.17±0.19 μg C L^{-1} h^{-1}) in June.

Particulate and sedimentary C and N stable isotopic ratios and contribution of organic matter sources to POM and SOM

The $\delta^{13}C$ signature of POM ranged between −26.49‰ (St. 2C, April) and −21.75‰ (St. 1I, June, Fig. 3a, Table S1), and values were distinct among sampling seasons and stations

Table 1 Physical-chemical parameters measured in the water column at the three stations and three sampling periods: temperature (Temp), oxygen saturation (%O2), salinity, PAR irradiance measured in the water column (E0), surface PAR irradiance measured in the air (Eref), the percentage of measured PAR irradiance in the water column with respect to surface PAR irradiance (%PAR), ratio between pheopigments and chlorophyll *a* (phaeo/chl *a*)

Sampling date	Station	Depth m	Temp °C	%O2	Salinity	E0 μEm^{-2} s^{-1}	Eref μEm^{-2} s^{-1}	%PAR	phaeo/chl *a*
11 Jun. 2013	St. 1E	1	22.8	114.8	36.1	1477.3	2486.4	59.4	0.72
		10	20.9	101.0	38.4	206.6	2486.4	8.3	0.31
13 Jun. 2013	St. 1I	1	21.4	102.0	36.3	1451.3	2443.3	59.4	0.49
		10	20.9	105.1	38.3	218.6	2453.7	8.9	0.44
15 Jun. 2013	St. 2C	1	23.5	113.6	36.2	1734.7	2343.8	74.0	2.44
		7	21.3	115.6	37.7	368.6	2347.2	15.7	0.56
05 Feb. 2014	St. 1E	1	12.0	NA	34.3	126.7	716.4	17.7	1.94
		10	13.2	NA	38.0	38.5	797.4	4.8	2.12
04 Feb. 2014	St. 1I	1	12.1	NA	36.3	134.3	466.1	28.8	1.48
		10	13.2	NA	38.3	22.6	460.1	4.9	3.71
03 Feb. 2014	St. 2C	1	12.2	NA	34.9	112.6	407.6	27.6	1.58
		7	12.8	NA	37.4	26.9	406.5	6.6	3.45
01 Apr. 2014	St. 1E	1	16.5	106.4	35.6	755.8	2108.9	35.8	1.04
		10	15.5	105.7	37.4	161.8	1971.1	8.2	1.19
03 Apr. 2014	St. 1I	1	17.0	105.3	35.6	396.4	2006.6	19.8	1.01
		10	15.7	110.4	37.5	146.9	1906.2	15.3	1.02
07 Apr. 2014	St. 2C	1	16.6	111.9	35.7	301.9	1576.6	19.2	0.54
		7	16.6	124.6	36.8	91.3	1318.0	6.9	0.99

(two-way ANOVA, $F_{2,24}$=17.58, p<0.001; $F_{3,24}$=3.30, p<0.05, respectively). $\delta^{13}C_{POM}$ was higher in June compared to April (Tukey's HSD test, p<0.01) and at St. 1I than at St. 2C (p<0.05). In the whole basin, $\delta^{15}N_{POM}$ ranged between 4.92‰ (St. 1E, June) and 9.81‰ (St. 2B, June) and values changed among seasons ($F_{2,24}$=7.16, p<0.005) and stations ($F_{3,24}$=12.64, p<0.001, Fig. 3b, Table S1). $\delta^{15}N$ data were higher in June and April compared to February (Tukey's HSD test, p<0.01) and higher at St. 2B than at the other stations (p<0.01, Fig. 3b, Table S1). The average C/N ratio of POM was 6.90±0.41 and did not change among seasons and stations (Table S1). $\delta^{13}C$ values in POM were generally

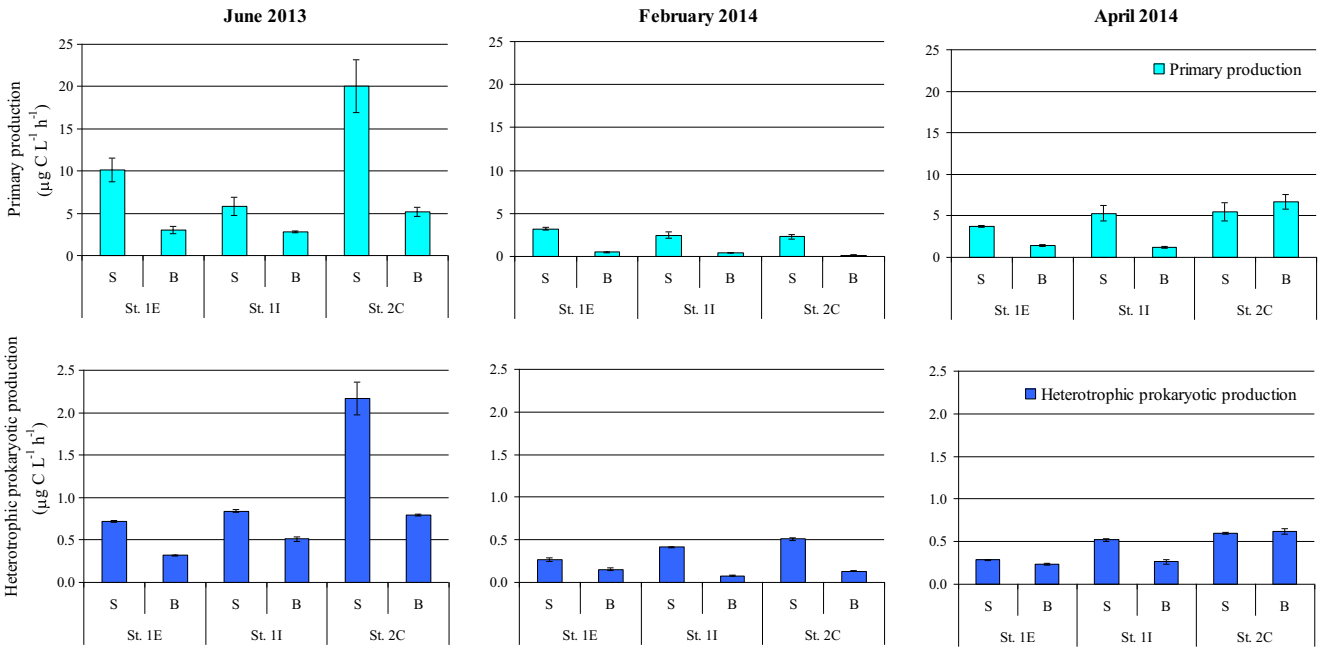

Fig. 2 Primary production and heterotrophic prokaryotic production at the three sampling stations in the three study periods

Table 2 Primary production measured at the sampling stations in the three study periods

Sampling date	Station	Depth	PP chl^{-1} μg C μg chl $a^{-1}h^{-1}$	PPa mg C m^{-2} h^{-1}
11 Jun. 2013	St. 1E	1	5.65	6.59
		10	2.03	
13 Jun. 2013	St. 1I	1	4.27	4.32
		10	1.95	
15 Jun. 2013	St. 2C	1	10.92	12.62
		7	4.93	
05 Feb. 2014	St. 1E	1	3.50	1.87
		10	0.82	
04 Feb. 2014	St. 1I	1	2.86	1.44
		10	1.15	
03 Feb. 2014	St. 2C	1	2.05	1.20
		7	0.24	
01 Apr. 2014	St. 2E	1	2.13	2.58
		10	1.11	
03 Apr. 2014	St. 2I	1	2.46	3.24
		10	0.98	
07 Apr. 2014	St. 2C	1	2.21	6.09
		7	1.81	

PP chl^{-1} chl *a*-normalized photosynthetic rates, *PPa* phytoplankton production areal rates

lower than in SOM (*t* test, t=4.58, df=11, p<0.001) while no differences were observed for $\delta^{15}N$ (Fig. 3 and Table S1).

The $\delta^{13}C$ isotopic ratio of SOM ranged between −22.98‰ (April, St. 1I) and −20.09‰ (April, St. 2B) and did not show appreciable seasonal variations (Fig. 3a, Table S1). However, differences were observed among stations (one-way ANOVA, $F_{3,8}$=14.47; p<0.01). $\delta^{13}C_{SOM}$ at St. 2B was higher than at the other stations (Tukey's HSD test, p<0.01). The $\delta^{15}N$

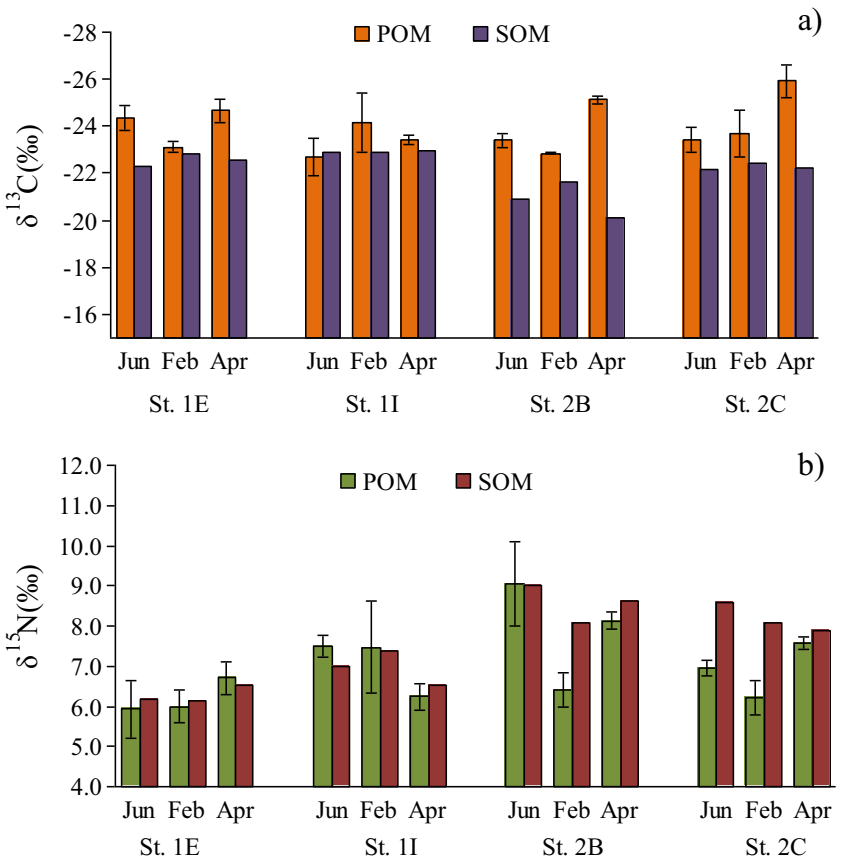

Fig. 3 Average values of $\delta^{13}C$ (**a**) and $\delta^{15}N$ (**b**) of POM and SOM at each sampling station and season. The *y*-axis begins with a value of −16 in **a** and 4 in **b** to better highlight variations among stations and months. Values are shown in Table S1, supplementary material

values of SOM ranged between 6.12‰ (St. 1E, February) and 9.00‰ (St. 2B, June, Fig. 3b). $\delta^{15}N$ isotopic ratio did not show a seasonal trend but changed among stations ($F_{3,8}$= 23.67, p<0.001). St. 2B and 2C displayed higher values than St. 1E and St. 1I (Tukey's HSD test, p<0.01, Fig. 3b and Table S1).

The C/N ratio in SOM ranged between 6.55 (St. 1E, February) and 17.13 (St. 1E, April) and did not change among seasons and stations (Table S1). The C/N ratio of SOM (12.14 ±2.85) was higher than C/N_{POM} (t=2.43, df=10, p<0.05, Table S1).

Results of the stable isotope mixing model (SIAR) suggested that terrestrial/riverine POM mainly contributed (45.5 %) to POM pools at all sampling stations and months (Fig. 4a, Table S2).

Such contribution was slightly higher during April and reached its maximum at St. 1E (mean contribution 54 %). Phytoplankton only contributed up to 29 % at St. 2B in February. Contribution from sewage sources peaked at St. 2B in June and April (Fig. 4a, Table S2). As expected, SOM resulted a more homogeneous mix of organic inputs (Fig. 4b). Comparatively, a higher contribution of terrestrial/riverine POM was evident in the sediments of the first inlet while the influence of sewage matter was higher in the second one. Notably, the contribution of macroalgae to the sediment pool increased up to 30–35 % in June and April at St. 2B.

Macroalgal coverage

According to the map obtained by high-resolution multispectral satellite remote sensing, the south-eastern area of the second inlet was the most densely colonized by macroalgae, while in the first inlet, a much lower areal coverage was observed. Different green macroalgae were observed by divers in the second inlet, mostly *C. prolifera* and *Caulerpa racemosa* but also *Chaetomorpha* sp. that were occasionally trapped in a van Veen grab or occurred in our sediment cores. Coverage percentages resulted to be 0 % at St. 1E; 10–15 % at

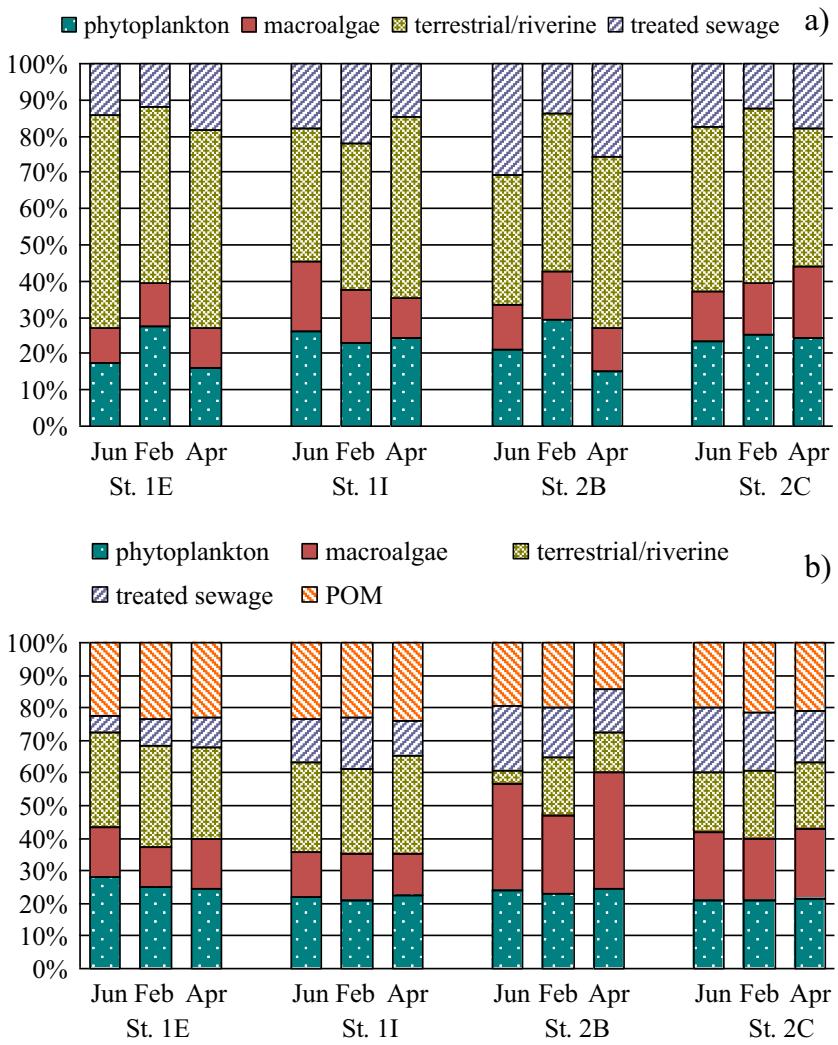

Fig. 4 Output of the mixing model (SIAR) showing **a** the mean percentage of contribution of potential organic matter sources to the particulate organic matter (POM) pool and **b** to the sediment organic matter (SOM) pool. Values (mean, and 95 % confidence intervals) for each source are shown in Table S2 in the supplementary material

St. 1I; 30–40 % at St. 2C and 90–100 % at St. 2B with a very patchy distribution at this latter station (Fig. 1). P_{max} of *Caulerpa* sp. was 0.22 mg C m^{-2} h^{-1} at St. 1I, 0.52 mg C m^{-2} h^{-1} at St. 2C, whereas reached 1.42 mg C m^{-2} h^{-1} at the patchy colonized St. 2B.

Contaminants in surface sediments

In June, total PCB concentrations ranged from about 46.0 ng g^{-1} d.w. (St. 2B and 2C) to 1159.7 ng g^{-1} d.w. (St. 1I) and in April from 39.0 ng g^{-1} d.w. (St. 2C) to 1067.6 ng g^{-1} d.w. (St. 1I) (Table 3). PCB 153 resulted the most abundant congener that accounted for approximately 15–30 % of the total concentration (Table 3). PCB patterns were always dominated by hexachlorinated (ranging from 39.3 % at St. 1I in June to 58.5 % of the total load at St. 1E in April), pentachlorinated (from 21.0 % at St. 1E to 38.6 % at St. 2B, both in June) and heptachlorinated biphenyls (up to 30.1 % at St 1I in June), while the lower chlorinated congeners (trichlorobiphenyls and tetrachlorobiphenyls) generally represented a small (<5 %) contribution to the total concentration.

Overall, metal concentrations measured in surface sediments were higher in April than in June, except for Fe, Al and Cr (Table 4). Higher concentrations were obtained in sediments from the first inlet than those from the second one. In particular, As, Cu, Zn, Pb, Mn, Sn and Hg consistently displayed higher concentrations at St. 1E and St. 1I compared to those at St. 2B and St. 2C.

Multidimensional scaling and analysis of similarity

A good spatial separation of samples was obtained in the MDS both for surface (stress=0.05) and bottom data (stress=0.07) (Fig. 5a, b).

According to ANOSIM, significant differences were obtained among sampling periods both for surface (R_{ANOSIM}=0.658, p=0.1 %) and bottom samples (R_{ANOSIM}=0.456, p=0.1 %), between the two inlets (R_{ANOSIM}=0.195, p=2.6 % and R_{ANOSIM}=0.408, p=0.5 % for surface and bottom data, respectively) as well as among stations (R_{ANOSIM}=0.118, p=3.3 % and R_{ANOSIM}=0.173, p=0.9 % for surface and bottom data, respectively). The pairwise ANOSIM test performed on stations did not result significantly different for surface data, whereas the bottom of St. 2C was significantly different from both St. 1E (R_{ANOSIM}=0.224, p=2.1 %) and St. 1I (R_{ANOSIM}=0.181, p=3.8 %).

Table 3 PCB concentrations analysed at the four stations in June 2013 and April 2014, expressed as the sum of 28 PCB congeners, the sum of 7 target PCBs (∑PCB 28-52-101-118-153-138 and 180) and of the congener PCB153 that is commonly used as a proxy of the PCB concentration

PCBs (ng g^{-1} d.w.)	Sampling date	Stations			
		St. 1E	St. 1I	St. 2B	St. 2C
PCB ∑28	June 2013	551.8	1159.7	45.3	46.0
PCB ∑7target		280	590.7	24.3	22.5
PCB 153		84.1	167.3	9.0	8.5
PCB ∑28	April 2014	164.9	1067.6	164.8	39.0
PCB ∑7target		89.1	521.1	82.7	19.1
PCB 153		50.9	189.3	32.4	7.9

Discussion

Primary production and heterotrophic prokaryotic production in the Mar Piccolo

In this study, for the first time, we measured PP and heterotrophic HPP in the Mar Piccolo of Taranto. PP values were well above 2 μg C L^{-1} h^{-1} also during winter indicating that the Mar Piccolo is a quite productive basin. Values were strongly influenced by light availability in the water column, as demonstrated by the highly significant correlation with the PAR irradiance (R=0.76, p<0.001, Table 1). Due to the high phytoplankton production, the basin was oversaturated in oxygen, as confirmed by the oxygen profiles registered in the water column in two sampling periods (Table 1).

PP rates were highly correlated with chl *a* concentrations (R=0.80, p<0.001). The relatively high phaeo/chl *a* ratios (1.5 at the surface layer and up to 3.7 at the bottom) observed in February suggested that in that month, the phytoplankton assemblage was in the senescent phase. Interestingly, the phytoplankton assemblage responsible for the highest PP rate estimated in June in the second inlet was presumably also in a senescent phase, as indicated by a phaeo/chl *a* ratio of 2.44.

The sinking degrading phytoplankton represent highly palatable substrata for heterotrophic prokaryotes and could have fueled HPP rates that peaked in June 2013. Moreover, the high abundance of small diatoms observed in this period (Karuza et al. 2015 this issue) could have been responsible for a major availability of labile exudates (Hoagland et al. 1993), which stimulate the prokaryotic growth. HPP rates were further tightly related to the concentrations of both the particulate and dissolved organic matter (POC and DOC) in the water column (R=0.81, p<0.001 with POC and R=0.73, p<0.01 with DOC). In particular, in June 2013, DOC varied between 1.273 and 1.587 mg L^{-1} at the bottom of St. 2C and St. 1E, respectively. On the other hand, in April 2014, it ranged from 0.902 mg L^{-1} at the bottom of St. 1E to 1.963 mg L^{-1} at the surface of St. 2C (Kralj et al. 2015 this issue). The extracellular release

Table 4 Concentrations of the 13 heavy metals analysed at the four stations in June 2013 and April 2014

Stations	Sampling date	As	Cd	Cr	Cu	Fe	Ni	Zn	Pb	Al	V	Mn	Sn	Hg
mg kg^{-1} d.w.														
St. 1E	June 2013	15.05	0.87	35.50	34.86	16590	26.90	135	50	27774	47	189.08	6.91	0.90
St. 1I		17.16	0.90	26.44	56.69	22570	27.40	189	100	21499	51	163.39	7.86	1.62
St. 2B		11.90	0.90	26.76	25.80	17894	25.67	99	23	26923	49	136.36	2.48	0.60
St. 2C		11.03	0.99	32.09	25.66	21800	27.02	108	21	32942	55	125.89	1.99	0.30
St. 1E	April 2014	19.66	1.06	13.03	180.35	16136	43.59	231	80	18231	74	382.55	10.57	1.34
St. 1I		26.45	1.40	25.99	100.48	33840	59.28	319	152	16838	109	375.74	14.84	5.74
St. 2B		17.40	1.60	59.70	64.91	40760	63.22	222	74	25705	128	320.66	6.36	0.49
St. 2C		17.44	2.64	48.52	55.19	26944	63.94	180	51	25168	122	335.65	4.02	0.10

of recently fixed photosynthate contributes to the production of DOC in marine ecosystems and is particularly important for the trophic ecology of the plankton. The released compounds are susceptible to rapid uptake by heterotrophic bacteria, giving way to a linkage between primary and bacterial production that is essential for the cycling of matter through the microbial loop and the microbial food web (Marañón et al. 2004). Indeed, considering the entire study period, our PP and HPP hourly rates exhibited exactly the same pattern (Fig. 2), and their correlation was highly significant ($R=0.90$, $p<0.001$). Our mean PP/HPP ratio was 20.96, and excluding one outlier, it varied between 7.09 and 29.89. Previously, Puddu et al. (1998) demonstrated that in the northern Adriatic, the bacterial mediated processes are tightly coupled with the phytoplankton production. They reported that a very high percentage (40–80 %) of the carbon fixed by the phytoplankton has been requested for bacterial metabolism. Data of PP and HPP in the Mar Piccolo suggested that especially in June, these two processes were clearly in phase. Therefore, in this basin, the phototrophic plankton appear to be a main driving force in C-cycling, independently from their dimensional range and seasonal succession. The flow of C through the system seemed clearly shaped by two essential steps, i.e. the processes of primary production and OM degradation, quite active and efficient in the water column.

Higher PP and HPP rates in the second inlet are likely due to a major biomass of both autotrophic and heterotrophic organisms observed in the second inlet during our surveys (Karuza et al. 2015 this issue). Indeed, from 2002 onwards, higher plankton biomass in the second inlet has been well documented (Caroppo et al. 2012), mostly ascribable to its more lagoonal features. This inlet is shallower and characterized by a higher freshwater input and lower salinity compared to the first one (Cardellicchio et al. 2015 this issue) favouring the development of the phototrophic organisms in the water column. Although mussels that cover two thirds of the second inlet sequestrate a good part of the available biomass (Caroppo et al. 2012), the remaining fraction is still higher compared to that of the first inlet. We infer that a possible co-factor responsible for both the overall lower phytoplankton biomass and PP and HPP rates in the first inlet may be the higher concentration of contaminants in its surface sediments. Through resuspension, these contaminants could be temporarily transferred to the water column, entering the pelagic trophic web and interfering with the proper functioning of the pelagic ecosystem. Several studies have reported detrimental effects of contaminants on phytoplankton (Caroppo et al. 2006; Lafabrie et al. 2013a; Tiano et al. 2014) and photosynthesis (Pérez et al. 2006) in association with increased respiration rates (Lafabrie et al. 2013b).

In order to have an overview of the PP and HPP in the entire basin, the rates measured in the water column were integrated to those obtained in surface sediments (Table 5) (Franzo et al. 2015 this issue; Rubino et al. 2015 this issue). Since we estimated benthic processes only in June 2013 and April 2014, an integration was possible only in these two sampling periods. Primary and heterotrophic prokaryotic production rates obtained in the water column (PPw, HPPw) were converted from μg C L^{-1} h^{-1} to mg C m^{-2} h^{-1} and added to those estimated in surface sediments (PPs, HPPs) to have an evaluation of the total rates (PPi, HPPi) at the three sampled stations in the Mar Piccolo (Table 5).

PPw values were always much higher than PPs ones. The highest contribution of PPs to PPi was around 10.5 % and was calculated in the center of the first inlet in both sampling months. The lower PPs contribution was found at St. 1I close to the navy base. These total primary production rates (up to 12.86 mg C m^{-2} h^{-1}) are quite low for an enclosed shallow basin, such as the Mar Piccolo. In fact, considering the PP both in the water column and in the sediments, the microphytobenthos alone may contribute up to 50 % of the total PP in shallow coastal systems (Perissinotto et al. 2002; Montani et al. 2003). We suggest that low PPs rates in the Mar

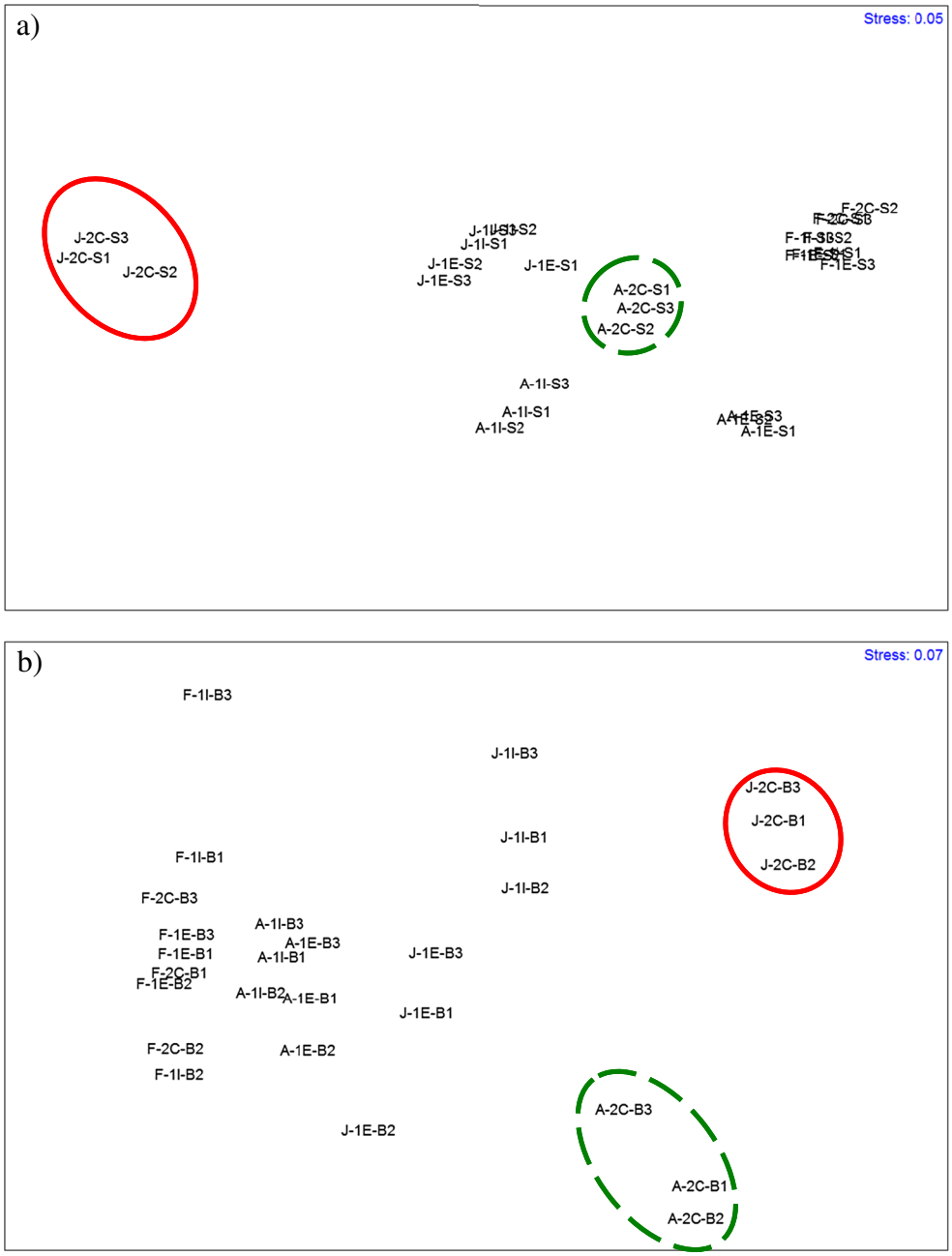

Fig. 5 Multidimensional scaling analysis (MDS) based on PP and HPP, abundances of autotrophic and heterotrophic picoplankton and autotrophic nanoplankton **a** at the surface (S) and **b** at the bottom layer (B). In **b**, also the $\delta^{15}N$ and $\delta^{13}C$ signatures of POM are included in the analysis. Replicated (n=3) samples are indicated per station (1E, 1I and 2C) and sampling month (*F* February, *A* April, *J* June). *Green dashed* and *red full circles* enclose April and June samples from the second inlet, respectively. February data are not clearly separated between inlets and thus are not enclosed in *circles*

Piccolo, especially at St. 1I, are likely ascribable to the high concentration of PCBs, heavy metals (Tables 3 and 4) and other contaminants accumulated in the sediments that can inhibit benthic PP and therefore interfere with the proper functioning of this ecosystem.

Yet, these estimates do not consider the contribution of macroalgae. At St. 1E, the bottom was unvegetated, as confirmed by the satellite map (Fig. 1), and therefore, no additional contribution had to be considered. At St. 1I, *Caulerpa* sp. with a P_{max} of 0.22 mg C m^{-2} h^{-1} could lead to an integrated value up to 4.60 mg C m^{-2} h^{-1} in June. At St. 2C, with a macroalgal contribution of about 0.52 mg C m^{-2} h^{-1}, the estimated total production of the system could reach 12.91 mg C m^{-2} h^{-1}. Overall, at the investigated stations, the phytoplankton is confirmed to be by far the most important primary producer in the Mar Piccolo.

The contribution of HPPs to HPPi was much higher in June than in April (Table 5). In June, the calculated rates in the water column and in the surface sediments were comparable, particularly at St. 1E, whereas HPPs contributed approximately for one third to HPPi at the other two stations. The low phaeo/chl *a* ratios observed in June at St. 1E re-enforce the idea that the higher rates could be boosted by the input of fresh organic matter from the water column as further indicated by

Table 5 Primary and heterotrophic prokaryotic production rates in the water column (PPw, HPPw), in surface sediments (PPs, HPPs) and as integrated rates (PPi, HPPi) at the three sampled stations and during the two sampling periods

	June 2013							
	PPw	PPs	PPi	PPs/PPw	HPPw	HPPs	HPPi	HPPs/HPPw
	mg C m^{-2} h^{-1}				mg C m^{-2} h^{-1}			
St. 1E	6.59	0.69	7.29	0.11	0.52	0.57	1.09	1.10
St. 1I	4.32	0.06	4.38	0.01	0.68	0.33	1.01	0.49
St. 2C	12.62	0.25	12.86	0.02	1.48	0.55	2.03	0.37
	April 2014							
	PPw	PPs	PPi	PPs/PPw	HPPw	HPPs	HPPi	HPPs/HPPw
	mg C m^{-2} h^{-1}				mg C m^{-2} h^{-1}			
St. 1E	2.58	0.27	2.85	0.10	0.26	0.10	0.36	0.41
St. 1I	3.24	0.13	3.37	0.04	0.39	0.05	0.44	0.14
St. 2C	6.09	0.50	6.59	0.08	0.61	0.16	0.77	0.27

the mixing model in which the plankton contribution to the SOM pool was slightly higher compared to the other months and stations. Conversely, an overall lower HPPs contribution to HPPi was obtained in April, especially at St. 1I (ca. 12 %).

Isotopic signature of POM and SOM and contribution of organic matter sources

Mean $\delta^{13}C$ (−23.90‰) of POM in the Mar Piccolo resulted comparable to values reported in the Lapalme and Venice lagoons (Berto et al. 2013; Carlier et al. 2007) and in the bay of Marseille (Cresson et al. 2012) and lower than those reported for other Mediterranean coastal surface waters and lagoons (Mazzola et al. 1999; Vizzini and Mazzola 2003). POM was highly ^{13}C depleted when compared to the typical signature of marine phytoplankton indicating the predominance of allochthonous sources of terrestrial origin (Cresson et al. 2012; Harmelin-Vivien et al. 2008). This result was confirmed by the SIAR model which showed a contribution (up to 54 %) of terrestrial/riverine POM to the entire pool. The ^{13}C depleted signal was more pronounced during April and could reflect high late-winter land run-off or freshwater intrusion which is one of the main features of this basin (Cardellicchio et al. 2015 this issue). $\delta^{15}N_{POM}$ values in the Mar Piccolo were comparable to those reported by Cresson et al. (2012) in the bay of Marseille. Both $\delta^{15}N$ values and the SIAR model clearly reflected a major nutrient enrichment of the second inlet (higher $\delta^{15}N$ values detected during June and April at St. 2B for POM and at St. 2B and 2C for SOM) compared to the first inlet. This enrichment could be due, as suggested by the mixing model, to the input of wastewater nutrients or alternatively to the organic matter derived from animal waste from the nearby mussel farming area (Owens 1985; Vander Zanden and Rasmussen 2001; Vizzini and Mazzola 2004) which covers two thirds of the surface of the second inlet. The measurement of specific end-members for the mussel farm activities (faecal material, biodeposits) will help to resolve this issue.

Impact of contaminated-sediment resuspension on the ecosystem functioning

At the four investigated sites, PCBs displayed dissimilar seasonal patterns. Particularly in April, PCB concentrations increased at St. 2B while they decreased at St. 1E. This could be attributed to natural and anthropogenic disturbance events that cause episodic sediment resuspension present in these areas of the basins and that lead to changes in the chemical properties of sediments. High levels of PCBs measured in the sediments of St. 1I obtained in this study are in agreement with previous reports in which this area is described as a major source of PCBs for the Mar Piccolo of Taranto (Cardellicchio et al. 2007). The general uniformity in the PCB pattern found in the surface sediments of the Mar Piccolo suggests that the contamination source was probably the same in all the investigated sites, likely related to the navy arsenal activities. In particular, considering the sum of the seven target PCBs, PCB 153 alone accounted for 57 % of their concentration, followed by PCB 138 and PCB 180, a pattern that is in agreement with previously reported data (Gómez-Lavín et al. 2011; Okay et al. 2009; Secco et al. 2005).

We obtained higher concentrations of most of the analysed metals in sediments of the first inlet compared to those of the second one. Our findings are in agreement with the results of Calace et al. (2005) and Cardellicchio et al. (2009), who reported that the first inlet of the Mar Piccolo is more contaminated by metals than the second one. These derive partially from the seawater coming from the Mar Grande through the two channels (in turn influenced by industrial wastewaters) but, to a much greater extent, from the presence of shipbuilding activities of the main Italian navy base, located in the first inlet. The frequent passage of navy ships and submarines in the centre of the first inlet, where the maximum depth reaches 13 m, likely resuspend the first centimetres of sediments that from the deeper layers reach the surface. In these subsurface layers, due to anoxic conditions and the presence of hydrogen sulphide, metals are present in the form of insoluble sulphurs,

tightly linked to the organic matter (Caroppo and Cardellicchio 1995). Once at the surface, under oxic conditions, a fraction of metals could change the oxidation state becoming more bioavailable and facilitating, therefore, their entry into the pelagic food web.

Overall, higher concentrations of As, Cu, Zn, Pb, Mn, Sn and Hg were observed in April compared to June data. Also considering a certain degree of spatial variability that may have occurred during sampling, metal concentrations were consistently higher at the four stations in April. These great differences between the two sampling periods (up to more than twice) may be attributable to phytoplankton dynamics (Heimbürger et al. 2010). According to these authors, higher metal concentrations in the water column coincide with blooms of nanophytoplankton and picophytoplankton because they accumulate more efficiently particle-reactive trace metals, especially Hg, due to their greater surface/volume ratio compared to microphytoplankton. Therefore, we can infer that our lower metal concentrations in surface sediments in June may be attributed to a partial sequestration of these compounds by nanophytoplankton that reached up to $1.3\times10^{7}\pm 5.9\times10^{5}$ cells L^{-1} in that month (Karuza et al. 2015 this issue).

To date, the effects of resuspension of contaminated sediments on pelagic organisms and ecosystem functioning remain underresearched (Lafabrie et al. 2013a). For instance, the processes of PCB transfer at the lowest trophic levels are poorly understood, and the mechanisms of PCBs uptake by plankton are still a matter of scientific discussion (Tiano et al. 2014). Our results provide new insights into these open questions as summarized in the MDS outputs. The pelagic system functioning seems to be variably influenced by resuspension events according to the season and the depth. In Fig. 5b, in June, St. 2C was clearly separated from the other sites suggesting a different environmental situation than that in the first inlet. The stratification of the water column that began in early summer probably slowed down the water exchange between the two inlets and enhanced the confinement characteristics of the second one. In contrast, February samples were not well separated, following the winter mixing of the water column while the intermediate position of April samples seems to corroborate the hypothesis of the gradual decrease of naturally induced sediment resuspension from winter towards early summer. On the other hand, the MDS performed on surface data (Fig. 5a) suggests that the effects of resuspended contaminants on the pelagic system could vary according to the distance from their main source, i.e. the sediments. Surface samples, in fact, did not show a clear separation among stations and/or inlets suggesting that at the surface, even the most impacted site was comparable to the others. This hypothesis is also confirmed by the pairwise ANOSIM test performed on stations separating surface from bottom samples. While at the surface the stations were not significantly different among each other, the bottom of St. 2C was significantly different from both St. 1E (R_{ANOSIM}=0.224, p=2.1 %) and St. 1I (R_{ANOSIM}=0.181, p=3.8 %).

Conclusion

In this study, for the first time, phytoplankton PP and HPP were measured in the Mar Piccolo of Taranto and used as proxies of the ecosystem functioning. This semi-enclosed basin resulted quite productive over the study period. Considering the three major primary producers (phytoplankton, microphytobenthos and macroalgae), the phytoplankton resulted by far the most important primary producer at the investigated sites. This was also confirmed by the SIAR model that, although indicating an overall major contribution of allochthonous material of terrestrial origin to the POM pool, pointed to a more pronounced contribution of phytoplankton compared to that of macroalgae. The contribution of macroalgae to the sediment pool was higher in one site of the second inlet densely colonized by macroalgae, as confirmed by the satellite map of the seabottom.

Over the study period, PP and HPP data exhibited exactly the same pattern, indicating that the heterotrophic prokaryotes were boosted by the extracellular release of recently fixed photosynthates and degrading phytoplankton cells. In spring and early summer, significantly lower PP and HPP rates were found in the first inlet compared to the second one, suggesting a detrimental effect of contaminants which could be resuspended from the heavily polluted sediments of the navy arsenal and spread over the whole first inlet. However, their interference with the proper functioning of the pelagic ecosystem seems to be limited to the bottom layers.

Acknowledgments The activities described in this publication were funded by the Project Bandiera RITMARE—La Ricerca Italiana per il Mare coordinated by the National Research Council and funded by the Ministry for Education, University and Research within the National Research Programme 2011–2013. We thank Dr. Cassin for the map of the main pressures and the anonymous reviewers for their constructive criticism that greatly improved the paper.

References

Bernardeau-Esteller J, Marín-Guirao L, Sandoval-Gil JM, Ruiz JM (2011) Photosynthesis and daily metabolic carbon balance of the invasive *Caulerpa racemosa* var. *cylindracea* (Chlorophyta: Caulerpales) along a depth gradient. Sci Mar 75:803–810. doi:10.3989/scimar.2011.75n4803

Berto D, Rampazzo F, Noventa S, Cacciatore F, Gabellini M, Bernardi Aubry F, Girolimetto A, Boscolo Brusà R (2013) Stable carbon and nitrogen isotope ratios as tools to evaluate the nature of particulate organic matter in the Venice lagoon. Estuar Coast Shelf Sci 135:66–76. doi:10.1016/j.ecss.2013.06.021

Bongiorni L, Fiorentino F, Auriemma R, Bernardi Aubry F, Camatti E, Camin F, Nasi F, Pansera M, Ziller L, Grall J (2015) Food web

structure of a confined and heavily affected coastal basin (the Mar Piccolo of Taranto) revealed by carbon and nitrogen stable isotopes analyses. This issue

Borfecchia F, De Cecco L, Martini S, Ceriola G, Bollanos S, Vlachopoulos G, Valiante LM, Belmonte A, Micheli C (2013a) *Posidonia oceanica* genetic and biometry mapping through high-resolution satellite spectral vegetation indices and sea-truth calibration. Int J Remote Sens 34:4680–4701. doi:10.1080/01431161.2013.781701

Borfecchia F, Micheli C, Carli F, De Martis SC, Gnisci V, Piermattei V, Belmonte A, De Cecco L, Martini S, Marcelli M (2013b) Mapping spatial patterns of *Posidonia oceanica* meadows by means of daedalus ATM airborne sensor in the coastal area of Civitavecchia (Central Tyrrhenian Sea, Italy). Remote Sens 5:4877–4899. doi:10.3390/rs5104877

Calace N, Ciardullo S, Petronio BM, Pietrantonio M, Abbondanzi F, Campisi T, Cardellicchio N (2005) Influence of chemical parameters (heavy metals, organic matter, sulphur and nitrogen) on toxicity of sediments from the Mar Piccolo (Taranto, Ionian Sea, Italy). Microchem J 79:243–248. doi:10.1016/j.microc.2004.10.005

Cardellicchio N, Buccolieri A, Giandomenico S, Lopez L, Pizzulli F, Spada L (2007) Organic pollutants (PAHs, PCBs) in sediments from the Mar Piccolo in Taranto (Ionian Sea, Southern Italy). Mar Pollut Bull 55:451–458. doi:10.1016/j.marpolbul.2007.09.007

Cardellicchio N, Buccolieri A, Leo AD, Librando V, Minniti Z, Spada L (2009) Methodological approach for metal pollution evaluation in sediments collected from the Taranto Gulf. Toxicol Environ Chem 91:1273–1290. doi:10.1080/02772240802616494

Cardellicchio N, Annicchiarico C, Di Leo A, Giandomenico S, Spada L (2015) The Mar Piccolo of Taranto: an interesting ecosystem for the study of the environmental problems. This issue

Carlier A, Riera P, Amouroux J-M, Bodiou J-Y, Escoubeyrou K, Desmalades M, Caparros J, Grémare A (2007) A seasonal survey of the food web in the Lapalme Lagoon (northwestern Mediterranean) assessed by carbon and nitrogen stable isotope analysis. Estuar Coast Shelf Sci 73:299–315. doi:10.1016/j.ecss.2007.01.012

Caroppo C, Cardellicchio N (1995) Preliminary study on phytoplankton communities of Mar Piccolo in Taranto (Jonian Sea). Oebalia 21:61–76

Caroppo C, Stabili L, Aresta M, Corinaldesi C, Danovaro R (2006) Impact of heavy metals and PCBs on marine picoplankton. Environ Toxicol 21:541–551. doi:10.1002/tox.20215

Caroppo C, Giordano L, Bellio G, Bisci AP, Palmieri N, Portacci G, Sclafani P, Hopkins TS (2012) Progress toward sustainable mussel aquaculture in Mar Piccolo, Italy. Ecol Soc 17(3):10. doi:10.5751/ES-04950-170310

Cibic T, Virgilio D (2011) In situ primary production measurements as an analytical support to remote sensing—an experimental approach to standardize the 14C incorporation technique. INTECH Open Access Publisher

Cibic T, Blasutto O, Burba N, Fonda Umani S (2008) Microphytobenthic primary production as ^{14}C uptake in sublittoral sediments of the Gulf of Trieste (northern Adriatic Sea): methodological aspects and data analyses. Estuar Coast Shelf Sci 77:113–122. doi:10.1016/j.ecss.2007.09.005

Cibic T, Franzo A, Celussi M, Fabbro C, Del Negro P (2012) Benthic ecosystem functioning in hydrocarbon and heavy-metal contaminated sediments of an Adriatic lagoon. Mar Ecol Prog Ser 458:69–87

Cole JJ, Findlay S, Pace ML (1988) Bacterial production in fresh and saltwater ecosystems: a cross-system overview. Mar Ecol Prog Ser 43:1–10

Cresson P, Ruitton S, Fontaine M-F, Harmelin-Vivien M (2012) Spatio-temporal variation of suspended and sedimentary organic matter quality in the Bay of Marseilles (NW Mediterranean) assessed by biochemical and isotopic analyses. Mar Pollut Bull 64:1112–1121. doi:10.1016/j.marpolbul.2012.04.003

Di Leo A, Annicchiarico C, Cardellicchio N, Giandomenico S, Conversano M, Castellano G, Basile F, Martinelli W, Scortichini G, Spada L (2014) Monitoring of PCDD/Fs and dioxin-like PCBs and seasonal variations in mussels from the Mar Grande and teh Mar Piccolo of Taranto (Ionian Sea, Southern Italy). Environ Sci Pollut Res 21:13196–131207. doi:10.1007/s11356-014-2495-6

Di Leo A, Annicchiarico C, Cardellicchio N, Cibic T, Giandomenico S, Spada L (2015) Mobilization of PCBs and heavy metals from contaminated marine sediments of the Mar Piccolo in Taranto during simulated resuspension experiment. This issue

Dubois S, Savoye N, Grémare A, Plus M, Charlier K, Beltoise A, Blanchet H (2012) Origin and composition of sediment organic matter in a coastal semi-enclosed ecosystem: an elemental and isotopic study at the ecosystem space scale. J Mar Syst 94:64–73. doi:10.1016/j.jmarsys.2011.10.009

Franzo A, Auriemma R, Nasi F, Vojvoda J, Pallavicini A, Cibic T, Del Negro P (2015) Benthic ecosystem functioning in the severely contaminated Mar Piccolo of Taranto (Ionian Sea, Italy): focus on heterotrophic pathways. This issue

Gargas E (1975) A manual for phytoplankton primary production studies in the Baltic, vol 2. The Baltic Marine Biologist, Water Quality Institute, Hørsholm, pp 1–18

Gómez-Lavín S, Gorri D, Irabien A (2011) Assessment of PCDD/Fs and PCBs in sediments from the Spanish Northern Atlantic Coast. Water Air Soil Pollut 221:287–299. doi:10.1007/s11270-011-0790-0

Harmelin-Vivien M, Loizeau V, Mellon C, Beker B, Arlhac D, Bodiguel X, Ferraton F, Hermand R, Philippon X, Salen-Picard C (2008) Comparison of C and N stable isotope ratios between surface particulate organic matter and microphytoplankton in the Gulf of Lions (NW Mediterranean). Cont Shelf Res 28:1911–1919. doi:10.1016/j.csr.2008.03.002

Hedges JI, Stern JH (1984) Carbon and nitrogen determinations of carbonate-containing solids. Limnol Oceanogr 29:657–663. doi:10.4319/lo.1984.29.3.0657

Heimbürger L-E, Cossa D, Marty J-C, Migon C, Averty B, Dufour A, Ras J (2010) Methyl mercury distributions in relation to the presence of nano- and picophytoplankton in an oceanic water column (Ligurian Sea, North-western Mediterranean). Geochim Cosmochim Acta 74:5549–5559. doi:10.1016/j.gca.2010.06.036

Hoagland KD, Rosowski JR, Gretz MR, Roemer SC (1993) Diatom extracellular polymeric substances: function, fine structure, chemistry, and physiology. J Phycol 29:537–566. doi:10.1111/j.0022-3646.1993.00537.x

Karuza A, Caroppo C, Cerino F, Monti M, Stabili L, Camatti E, Cibic T, Paola Del Negro (2015) Planktonic trophic web in Mar Piccolo of Taranto (Ionian Sea, Italy). This issue

Katsanevakis S, Stelzenmüller V, South A, Sørensen TK, Jones PJS, Kerr S, Badalamenti F, Anagnostou C, Breen P, Chust G, D'Anna G, Duijn M, Filatova T, Fiorentino F, Hulsman H, Johnson K, Karageorgis AP, Kröncke I, Mirto S, Pipitone C, Portelli S, Qiu W, Reiss H, Sakellariou D, Salomidi M, van Hoof L, Vassilopoulou V, Vega Fernández T, Vöge S, Weber A, Zenetos A, ter Hofstede R (2011) Ecosystem-based marine spatial management: review of concepts, policies, tools, and critical issues. Ocean Coast Manag 54:807–820. doi:10.1016/j.ocecoaman.2011.09.002

Kennish M, Brush M, Moore K (2014) Drivers of change in shallow coastal photic systems: an introduction to a special issue. Estuar Coasts 37:3–19. doi:10.1007/s12237-014-9779-4

Kirchman D, K'nees E, Hodson R (1985) Leucine incorporation and its potential as a measure of protein synthesis by bacteria in natural aquatic systems. Appl Environ Microbiol 49:599–607

Kralj M, Comici C, De Vittor C, Alabiso G (2015) Physical-chemical characteristics of a Site of National Interest—the Mar Piccolo of Taranto (Ionian Sea). This issue

Lafabrie C, Garrido M, Leboulanger C, Cecchi P, Grégori G, Pasqualini V, Pringault O (2013a) Impact of contaminated-sediment resuspension on phytoplankton in the Biguglia lagoon (Corsica, Mediterranean Sea). Estuar Coast Shelf Sci 130:70–80. doi:10.1016/j.ecss.2013.06.025

Lafabrie C, Hlaili AS, Leboulanger C, Tarhouni I, Othman HB, Mzoughi N, Chouba L, Pringault O (2013b) Contaminated sediment resuspension induces shifts in phytoplankton structure and function in a eutrophic Mediterranean lagoon. Knowl Manag Aquat Ecosyst 410: 5(16). doi:10.1051/kmae/2013060

Lee CW, Kudo I, Yanada M, Maita Y (2001) Bacterial abundance and production and their relation to primary production in Funka Bay. Plankton Biol Ecol 48:1–9

Lorenzen C, Jeffrey S (1980) Determination of chlorophyll in seawater. Unesco Technical Papers in Marine Science 35

Manini E, Luna GM, Danovaro R (2004) Benthic bacterial response to variable estuarine water inputs. FEMS Microbiol Ecol 50:185–194. doi:10.1016/j.femsec.2004.06.011

Marañón E, Cermeño P, Fernández E, Rodríguez J, Zabala L (2004) Significance and mechanisms of photosynthetic production of dissolved organic carbon in a coastal eutrophic ecosystem. Limnol Oceanogr 49:1652–1666. doi:10.4319/lo.2004.49.5.1652

Mazzola A, Sarà G, Venezia F, Caruso M, Catalano D, Hauser S (1999) Origin and distribution of suspended organic matter as inferred from carbon isotope composition in a mediterranean semi-enclosed marine system. Chem Ecol 16:215–238. doi:10.1080/02757549908037647

Montani S, Magni P, Abe N (2003) Seasonal and interannual patterns of intertidal microphytobenthos in combination with laboratory and areal production estimates. Mar Ecol Prog Ser 249:79–91. doi:10.3354/meps249079

Odum EP (1983) Basic ecology. Saunders College Pub

Okay OS, Karacik B, Basak S, Henkelmann B, Bernhöft S, Schramm K-W (2009) PCB and PCDD/F in sediments and mussels of the Istanbul strait (Turkey). Chemosphere 76:159–166. doi:10.1016/j.chemosphere.2009.03.051

Ottersen G, Olsen E, van der Meeren GI, Dommasnes A, Loeng H (2011) The Norwegian plan for integrated ecosystem-based management of the marine environment in the Norwegian Sea. Mar Policy 35:389–398. doi:10.1016/j.marpol.2010.10.017

Owens NJP (1985) Variations in the natural abundance of ^{15}N in estuarine suspended particulate matter: a specific indicator of biological processing. Estuar Coast Shelf Sci 20:505–510. doi:10.1016/0272-7714(85)90092-7

Parnell AC, Inger R, Bearhop S, Jackson AL (2010) Source partitioning using stable isotopes: coping with too much variation. PLoS ONE 5, e9672. doi:10.1371/journal.pone.0009672

Pérez P, Estévez-Blanco P, Beiras R, Fernández E (2006) Effect of copper on the photochemical efficiency, growth, and chlorophyll *a* biomass of natural phytoplankton assemblages. Environ Toxicol Chem 25: 137–143. doi:10.1897/04-392r1.1

Perissinotto R, Nozais C, Kibirige I (2002) Spatio-temporal dynamics of phytoplankton and microphytobenthos in a South African temporarily-open estuary. Estuar Coast Shelf Sci 55:47–58. doi:10.1006/ecss.2001.0885

Phillips DL, Inger R, Bearhop S, Jackson AL, Moore JW, Parnell AC, Semmens BX, Ward EJ (2014) Best practices for use of stable isotope mixing models in food-web studies. Can J Zool 92:823–835. doi:10.1139/cjz-2014-0127

Puddu A, La Ferla R, Allegra A, Bacci C, Lopez M, Oliva F, Pierotti C (1998) Seasonal and spatial distribution of bacterial production and biomass along a salinity gradient (Northern Adriatic Sea). Eutrophication Planktonic Ecosyst Food Web Dyn Elemental Cycl Dev Hydrobiol 127:271–282. doi:10.1007/978-94-017-1493-8_22

Pugnetti A, Armeni M, Camatti E, Crevatin E, Dell'Anno A, Del Negro P, Milandri A, Socal G, Fonda Umani S, Danovaro R (2005) Imbalance between phytoplankton production and bacterial carbon demand in relation to mucilage formation in the Northern Adriatic Sea. Sci Total Environ 353:162–177. doi:10.1016/j.scitotenv.2005.09.014

Pugnetti A, Del Negro P, Giani M, Acri F, Aubry FB, Bianchi F, Berto D, Valeri A (2010) Phytoplankton–bacterioplankton interactions and carbon fluxes through microbial communities in a microtidal lagoon. FEMS Microbial Ecol 72(2):153–164. doi:10.1111/j.1574-6941.2010.00839.x

Rubino F, Cibic T, Belmonte M, Rogelja M (2015) Microbenthic community structure and trophic status of sediments in Mar Piccolo of Taranto (Mediterranean, Ionian Sea). This issue

Sanchez-Vidal A, Pasqual C, Kerhervé P, Heussner S, Calafat A, Palanques A, Durrieu de Madron X, Canals M, Puigc P (2009) Across margin export of organic matter by cascading events traced by stable isotopes, northwestern Mediterranean Sea. Limnol Oceanogr 54:1488–1500. doi:10.4319/lo.2009.54.5.1488

Secco T, Pellizzato F, Sfriso A, Pavoni B (2005) The changing state of contamination in the Lagoon of Venice. Part 1: organic pollutants. Chemosphere 58:279–290. doi:10.1016/j.chemosphere.2004.06.030

Smith DC, Azam F (1992) A simple, economical method for measuring bacterial protein synthesis rates in seawater using ^{3}H-leucine. Mar Microb Food Webs 6:107–114

Spada L, Annicchiarico C, Cardellicchio N, Giandomenico S, Di Leo A (2012) Mercury and methylmercury concentrations in Mediterranean seafood and surface sediments, intake evaluation and risk for consumers. Int J Hyg Environ Health 215:418–426. doi:10.1016/j.ijheh.2011.09.003

Steemann-Nielsen E (1952) The use of radio-active carbon (C^{14}) for measuring organic production in the sea. J Conseil 18:117–140. doi:10.1093/icesjms/18.2.117

Terrados J, Ros JD (1992) The influence of temperature on seasonal variation of *Caulerpa prolifera* (Forsskal) Lamouroux photosynthesis and respiration. J Exp Mar Biol Ecol 162:199–212. doi:10.1016/0022-0981(92)90201-K

Tiano M, Tronczyński J, Harmelin-Vivien M, Tixier C, Carlotti F (2014) PCB concentrations in plankton size classes, a temporal study in Marseille Bay, Western Mediterranean Sea. Mar Pollut Bull 89: 331–339. doi:10.1016/j.marpolbul.2014.09.040

Vander Zanden MJ, Rasmussen JB (2001) Variation in $\delta^{15}N$ and $\delta^{13}C$ trophic fractionation: implications for aquatic food web studies. Limnol Oceanogr 46:2061–2066. doi:10.4319/lo.2001.46.8.2061

Vizzini S, Mazzola A (2003) Seasonal variations in the stable carbon and nitrogen isotope ratios ($^{13}C/^{12}C$ and $^{15}N/^{14}N$) of primary producers and consumers in a western Mediterranean coastal lagoon. Mar Biol 142:1009–1018. doi:10.1007/s00227-003-1027-6

Vizzini S, Mazzola A (2004) Stable isotope evidence for the environmental impact of a land-based fish farm in the western Mediterranean. Mar Pollut Bull 49:61–70. doi:10.1016/j.marpolbul.2004.01.008